

# ELECTROCHEMICAL SYNTHESIS OF CuO AND TiO<sub>2</sub> NANOPARTICLES FOR DYE-SENSITIZED SOLAR CELLS

Ali A. Ahmed<sup>a\*</sup>, Aqeel M. Jreo Alduhaidahawi<sup>b</sup>

<sup>a</sup>*Ministry of Education, Rusafa Second Directorate of Education, Baghdad, Iraq*

<sup>b</sup>*Department of Chemistry, College of Science, Kufa University, Najaf, Iraq*

**Abstract:** Different standard methods have previously been used for the synthesis of nanoparticles that produce unhealthy waste. They are also considered unsafe and expensive methods. An alternative technology is needed to synthesize nanoparticles that consume less energy and are more environmentally friendly. In this research, CuO and TiO<sub>2</sub> nanoparticles have been synthesized, which produce good energy and no environmental pollution using an easy and fast method (electrochemical). Additionally, dye-sensitive solar cells (DSSCs) have been fabricated from CuO and TiO<sub>2</sub> nanoparticles, which were synthesized by a new green method, and the pigments methylene blue as a chemical dye and chlorophyll as a natural dye. These DSSCs were characterized by their high ability to absorb ultraviolet energy, where the efficiency of energy conversion ( $\eta$ ) of ITO-CuO was approximately 3.69 and 2.61% with methylene blue dye and chlorophyll dye, respectively, while the efficiency of ITO-TiO<sub>2</sub> was 3.20 with MB and 2.08% with chlorophyll. The results showed a significant progression of efficiency of energy conversion using methylene blue dye in both cells, and the DSSC using CuO was the best.

**Keywords:** DSSCs; electrochemical; nanoparticles; copper oxide; titanium dioxide

## Introduction

The dye-sensitized solar cells (DSSCs) studies have attracted several researchers since their invention.<sup>1</sup> Compared to silicon cells, DSSCs are

---

\*Ali A. Ahmed, *e-mail*: alia.alhussaini@student.uokufa.edu.iq

low-cost, not hazardous, and the environment is pollution-free. Accordingly, the technology of DSSCs is promising for harvesting solar energy. This could significantly reduce the world's energy demand.<sup>2</sup> In DSSCs, dye is used to harvest light and produce electrons, while titanium dioxide ( $\text{TiO}_2$ ) mimics carbon dioxide's role in photosynthesis.<sup>3</sup> A critical parameter affecting the efficiency of the cell is the dye's absorption on the surface of nanoparticles.<sup>4</sup> DSSCs consist of wideband semiconductors, selective dye, a conducting electrolyte, and two electrodes with opposite charges.<sup>5</sup> In addition, sensitizer dye is crucial to the functioning of DSSC, and semiconductor materials that fulfil these properties are  $\text{CuO}$ , and  $\text{TiO}_2$ .<sup>6</sup> Since  $\text{TiO}_2$  resists degradation under ultraviolet light.<sup>7</sup> The chemical absorption of pigment on nanoparticles of  $\text{CuO}$  and  $\text{TiO}_2$  plays an important role in solar cell efficacy.<sup>8</sup>

Standard pigments can be replaced by natural dyes found in the leaves of fruits, plants, vegetables, and flowers without appreciable loss in efficiency.<sup>9</sup> The non-toxicity of dye, availability, biodegradation capability, low cost, and efficiency make it suitable for application as dye-sensitized.<sup>10-12</sup> p-DSSC photocathodes with a higher dielectric constant and larger valence band gap were prepared using  $\text{CuO}$  nanoparticles.<sup>13</sup> The  $\text{CuO}$  and  $\text{TiO}_2$  nanoparticle powder can be made using a variety of techniques, including electrochemical precipitating, co-precipitation, sol-gel precipitation, solution combustion, and solid-state reactions. The electrochemical precipitating method, which is used in this work, produces nanoparticles quickly, easily, cheaply, at high purity, and in a very short time, not exceeding one day.<sup>14</sup> In this study, chlorophyll as a natural dye and methylene blue as a chemical dye were utilized to generate electricity by applying photovoltaic solar cells.<sup>15</sup>

Green synthesized copper oxide (CuO) nanoparticles (NPs), which were synthesized by the leaf extract of the *Calotropis gigantea* plant, were employed as electrocatalytic materials for the fabrication of counter electrodes in dye-sensitive solar cells (DSSCs), where solar to electrical energy conversion efficiency was ~3.4%.<sup>16</sup> In a previous study on the green manufacture of CuO nanoparticles using peppermint plant extract, the conversion energy efficiency was 3.3%.<sup>17</sup> A study claimed the effectiveness of the sensitive dye in solar cells, manufactured based on titanium oxide nanoparticles and using three dyes obtained from the *Begonia malabaricana* L. plant (BM), *Mela stoma malabathricum* (MM), and *Punica granatum* L. (POM). Experimental results showed that DSSCs sensitized with BM dye achieve the highest conversion efficiency of 1.76% compared to MM and POM dye, which have maximum efficiency of 0.76 and 1.12%, respectively.<sup>18</sup> In the study synthesizing titanium oxide nanoparticles and using sensitizers extracted from the natural sources of *Agaricus Bisporus* (mushroom) and *Citrus Limonium* (lemon) leaves, the efficiency of the solar cell was 0.54%.<sup>19</sup> the current study showed higher efficiency than the studies mentioned above.

## Experimental Section

### *Materials*

All materials and solvents utilized in this search were used as such without further purification, whereas titanium foil (99%) and copper foil (98%) were obtained from Baoji Jinsheng Metal Material Company. Potassium chloride (96%), polyvinyl alcohol (PVA), and graphite electrodes were supplied from Fluka Company, and graphite electrodes were obtained from Graphite India Limited Company. Acetone (98%), ethanol (99%), polyethylene glycol (PEG, 97%), and potassium iodide (97%) were provided

from CDH, and iodine (99%) was obtained from Thomas Baker. Deionized water (D.W.) was obtained from OneMed; methylene blue dye (98%) was obtained from Alfa Aesar; natural eucalyptus leaves and ITO glass ( $76.2 \times 25.4 \times 1.1$  mm, 11–15  $\Omega$ ) were obtained from Redox Me Company.

### *Instrumentation*

CuO and TiO<sub>2</sub> were characterised using X-ray diffraction analysis (XRD) (PANalytical AERIS) (operates at 600W (15mA and 40kV), fast Pixel3D 2-dimensional detector, 6 sample automatic sample changer, high-resolution expansion pack for improved resolution at low angles, 2" diameter sample holders, and scan parameters 0-90° (2 $\theta$ ), UV–vis diffuse reflectance spectroscopy (DRS) (Thermo Biomate 5 spectrophotometer a Double-beam, quartz-coated optic design with a wavelength range of 190-1100 nm, a wavelength accuracy of 1.0nm, and measure rates on up to 7 samples in parallel, with run times up to 40 hours, field emission scanning electron microscopy (FESEM) (INSPECT F50) (30kV: 1.0 nm maximum beam current: 200 nA, high vacuum X x Y x Z (mm): 50 x 50 x 50 mm, stage tilt -15° a 75°, and rotation: 360°), EDX (thermo Axia) (accelerating voltage range: 200 V – 30 k, magnification: 5 to 1,000,000 $\times$ , integrated current measurement: up to 2  $\mu$ A, continuously adjustable beam current range, and true sight X EDS detector. Solid angle 13 mSr, resolution 129 eV), and transmission electron microscopy (TEM) (EM 208S) (20-100 kV electron column, tungsten gun, twin objective lens, imaging modes: bright field, dark field, goniometer with single tilt holder PC, DOS OS, Philips UI, camera: CMOS 1.3 MP, vacuum system, and ODP with mechanical PVP).

### *Preparation of CuO nanoparticles*

The CuO nanoparticles were synthesized by the electrochemical method using the active electrode (anode), which is an electrode made of

copper foil, and the inert electrode (cathode), which is a graphite electrode, as shown in Figure 1. A power source was also used. The anode and cathode were cleaned with ethanol and acetone before being rinsed with D.W.<sup>20</sup> The electrochemical cell was filled with a 200.0 mL electrolyte solution consisting of 5 mL of 10% KCl and 10 mL of 10% PVA (stabilizer agent), and the remaining volume of the electrolyte solution was filled with deionized water. In addition, the active electrode consisted of connected pieces of copper foil (1 cm × 4 cm), which were placed face-to-face with a graphite electrode (2 cm × 5 cm) and subsequently immersed in the cell electrolyte.<sup>21</sup> The electrolysis process was carried out in an undivided electrolysis cell and stirred at 30 °C for about 60 min at 25 V. The CuO precipitate resulting from this process was centrifuged, rinsed several times with ethanol and D.W., and then placed in a drying oven, where it was dried for about 60 min. at 70 °C before being calcined at 700 °C for around 60 min.<sup>22</sup> In the same way, TiO<sub>2</sub> nanoparticles were synthesized, but titanium foil (1 cm x 4 cm) was used.

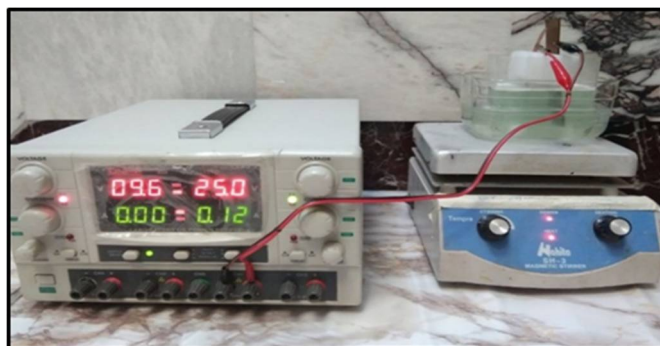


**Figure 1.** The electrochemical apparatus used to synthesize the CuO and TiO<sub>2</sub> nanoparticles

### *Fabrication of DSSCs*

ITO glass was carefully cleaned with ethanol and DW before being dried with air to remove impurities. The following method was used to

design a chemically and naturally dye-sensitive solar cell: a few drops of PEG were added to a small amount of nanoparticles ( $\text{CuO}$  or  $\text{TiO}_2$ ) to make a colloidal solution (photoanode). While the counter electrode was made of graphite powder and a few drops of PEG, the photoanode and the counter electrode were annealed at  $300\text{ }^\circ\text{C}$  for around 2 hours. The photoanode was placed in a chemical dye solution of 0.5% (w/v) MB by the same method, but another photoanode was put in a chlorophyll dye solution extracted from eucalyptus leaves.<sup>23</sup> Then both electrodes are placed in the dark for about 7–12 hours. Then, it is cleaned using ethanol and deionized water. Finally, 2–3 drops of an electrolyte solution of 0.1 M iodine (10 g of KI and 3.715 g of  $\text{I}_2$  in 250 ml deionized water) as shown in Figure 2 are placed between the two electrodes, and the solar cell efficiency is determined.<sup>24</sup>

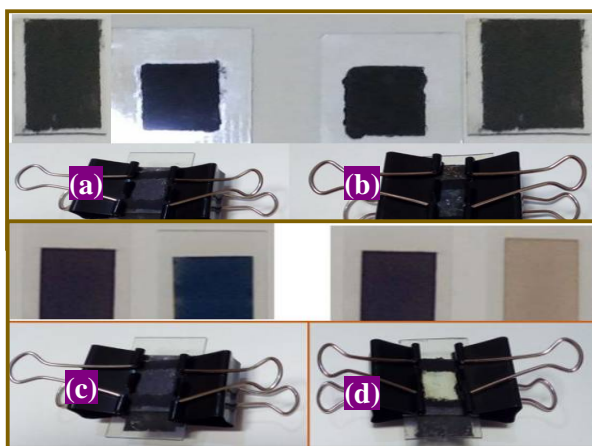


**Figure 2.** Design of (a)  $\text{CuO}$  MB, (b)  $\text{CuO}$  Chlorophyll, (c)  $\text{TiO}_2$  MB, and (d)  $\text{TiO}_2$  Chlorophyll dye DSSCs.

## Results and Discussions

### *X-ray diffraction Analysis for $\text{CuO}$ and $\text{TiO}_2$ Nanoparticles*

The XRD is used for the assessment of the phase purity and crystallinity of inorganic materials.<sup>25</sup> The XRD of  $\text{CuO}$  patterns suggests

that all diffraction peaks are in good agreement with the CuO standard diffraction data (JCPDS card no. 48-1548)<sup>26</sup> as shown in Figure 3a. the structure of CuO NPS was monoclinic (tenorite), while other diffraction data were appearances (JCPDS No. 89-4921)<sup>27</sup>, as shown in Figure 3b. TiO<sub>2</sub> was in anatase and rutile phases. The average crystal size of CuO and TiO<sub>2</sub> NPs can be calculated using Scherrer's equation 1, where it was 39.24 and 46.27 nm, respectively, because the variables of this equation obtained XRD data:

$$D = \frac{K\lambda}{FWHMCOS \theta} \quad (1)$$

where D is the size of the crystals,  $\theta$  is the Bragg diffraction angle, FWHM is the full width of the diffraction peak at half maximum,  $\lambda$  is the wavelength of Cu-K radiation (0.15406 nm), K is a constant and it is equivalent to 0.9.<sup>28</sup>

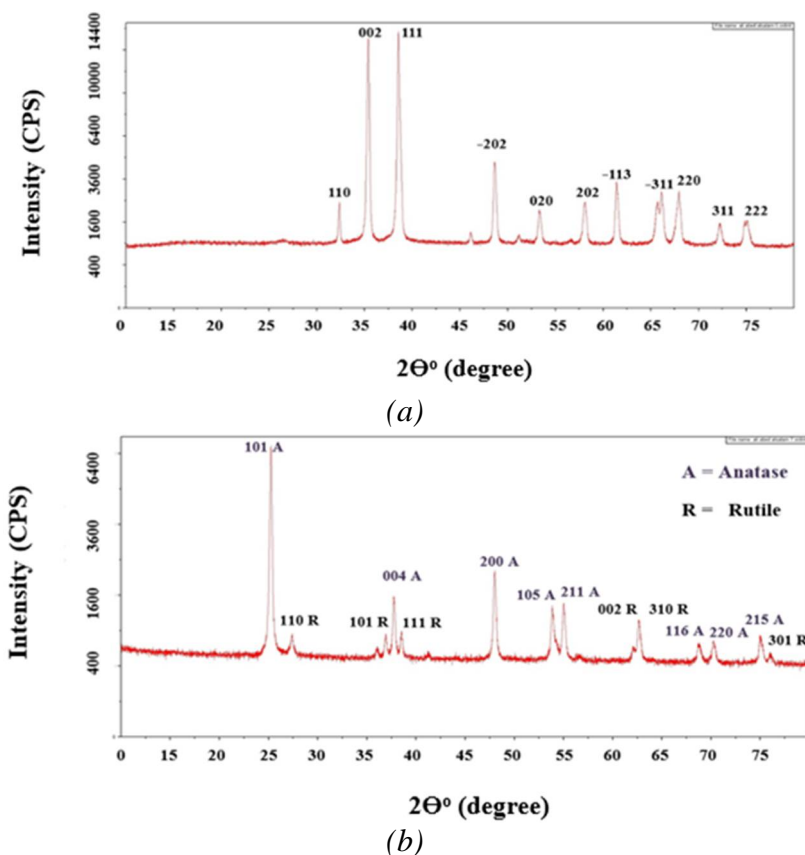


**Figure 3.** X-ray diffraction pattern of (a) CuO, and (b) TiO<sub>2</sub> nanoparticles

*TEM Analysis for CuO and TiO<sub>2</sub> Nanoparticles*

TEM microscopic images of CuO and TiO<sub>2</sub> nanoparticles provide evidence that the CuO nanoparticles have a cubic shape and a very small diameter. Moreover, the TiO<sub>2</sub> nanoparticles have a spherical shape. The statistical results showed that the average particle size of CuO and TiO<sub>2</sub> NPs at the 100 nm scale was 23.03 and 36.85 nm, respectively. This is further evidence for the preparation of CuO and TiO<sub>2</sub> nanoparticles, which is shown in Figure 4.

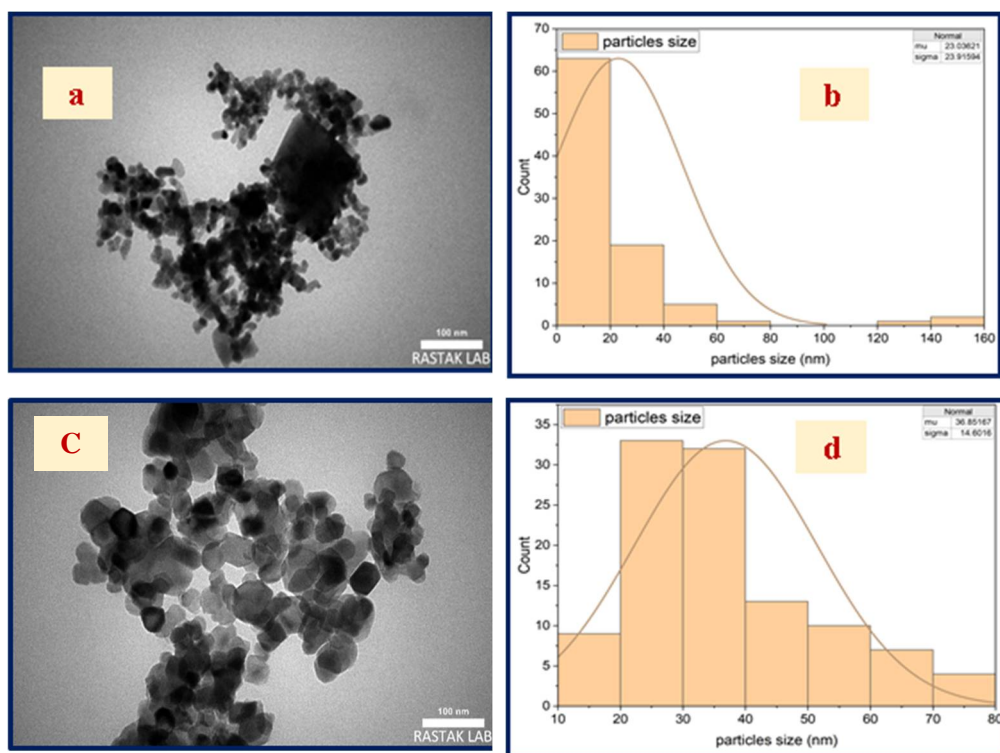


**Figure 4** TEM images and size distribution graphs at 100 nm scale of (a, b) for CuO, and (c, d) for TiO<sub>2</sub> nanoparticles.

*FESEM Analysis for CuO and TiO<sub>2</sub> Nanoparticles*

The morphology of CuO and TiO<sub>2</sub> nanoparticles was observed using FESEM. Figure 5 indicated that the nanoparticles were prepared in the nanometer range, and some of the nanoparticles were well separated from each other, while most of them were present in the agglomerated form of tiny crystals. This agglomeration is due to electrostatic effects.<sup>29</sup> Also, they provide evidence of CuO nanoparticle cubic morphology. While the TiO<sub>2</sub> nanoparticles have a spherical morphology, Statistical results showed that the mean particle sizes of CuO and TiO<sub>2</sub> nanoparticles at 500 nm were 75.13 and 79.10 nm, respectively.

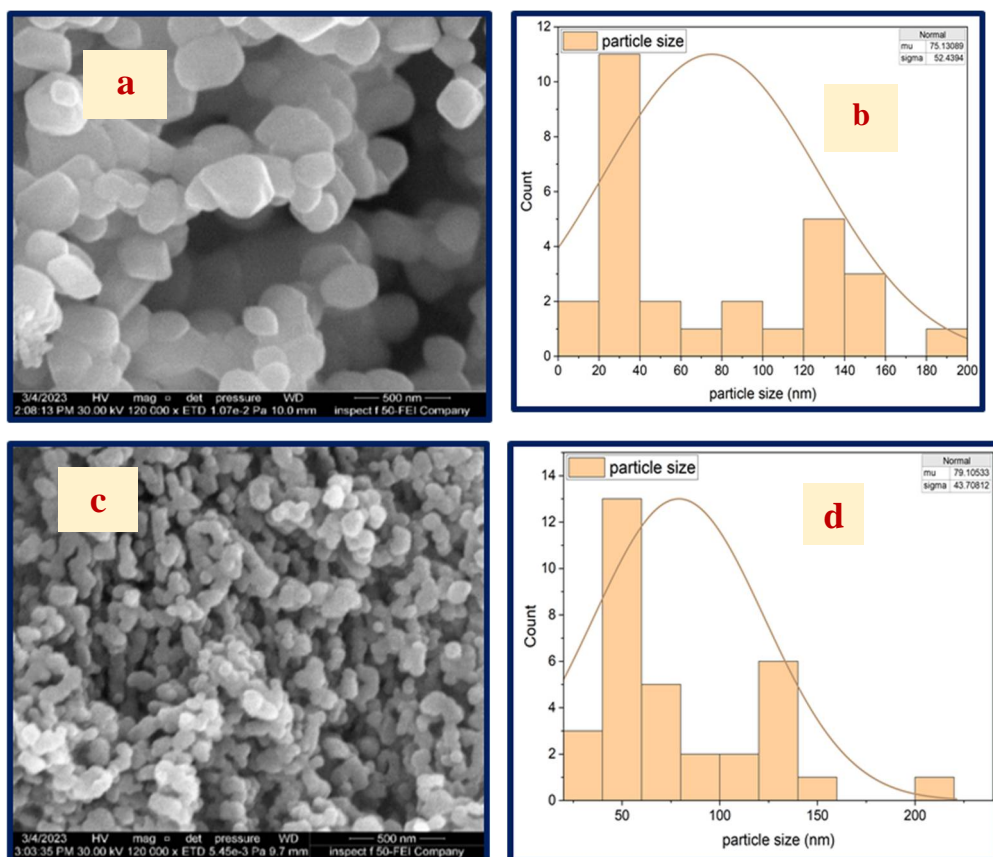


**Figure 5.** FESEM images and size distribution graphs at 500 nm scale of (a, b) for CuO, and (c, d) for TiO<sub>2</sub> nanoparticles.

### EDX Analysis for CuO and TiO<sub>2</sub> Nanoparticles

The purity, confirmed composition, distribution of the elements in the samples, and stoichiometry of the electrochemically produced CuO and TiO<sub>2</sub> nanoparticles were evaluated using EDX. Figure 6 reveals the presence of unique signals for oxygen, copper, and titanium, providing proof that there was a high level of purity in the samples.

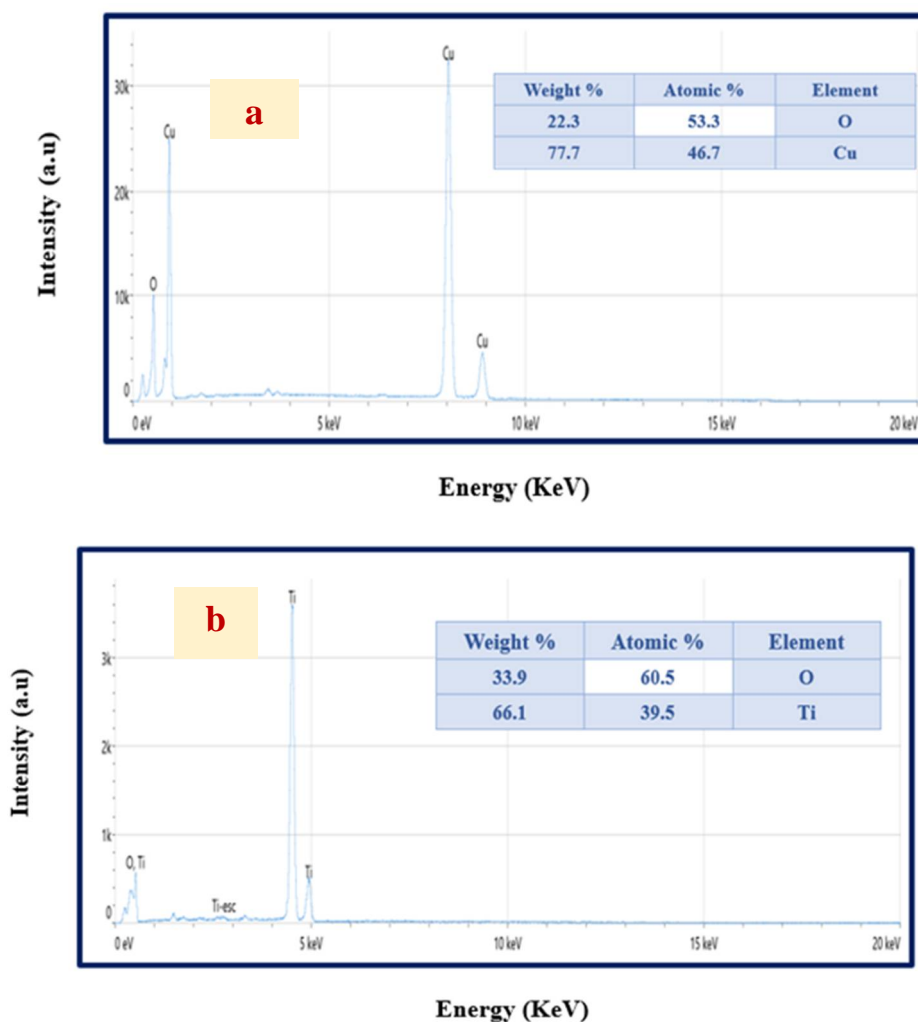


**Figure 6.** EDX spectrum of (a) CuO, and (b) TiO<sub>2</sub> nanoparticles

*UV-VIS DRS study of CuO and TiO<sub>2</sub> Nanoparticles*

Nanoparticles of thin films of CuO and TiO<sub>2</sub> were made on glass slides at room temperature and analyzed with solid-state UV-Visible spectroscopy. Figure 7 shows that the  $\lambda_{\text{max}}$  obtained was around 353 and 311 nm for CuO and TiO<sub>2</sub> respectively, and the energy band gap was calculated by the Tauc relation equation 2.<sup>30</sup>

$$\alpha h\nu^{1/n} = k(h\nu - E_g) \quad (2)$$

where K is a constant,  $\alpha$  is the molar extinction coefficient,  $h\nu$  is the incident photon energy in eV,  $E_g$  is the optical energy band gap, and  $n$ : index depends on the type of transition. The band gap was estimated from the intersection of the two lines part of  $(\alpha h\nu)^2$  Plots vs.  $h\nu$  on the  $h\nu$  axis. The equation is a direct band gap. Based on this equation, the bandgap values of CuO and TiO<sub>2</sub> are 1.74 and 3.15 eV, respectively, indicating that CuO and TiO<sub>2</sub> are semiconductor because the calculated energy gap values are less than 4.0 eV.<sup>31</sup>

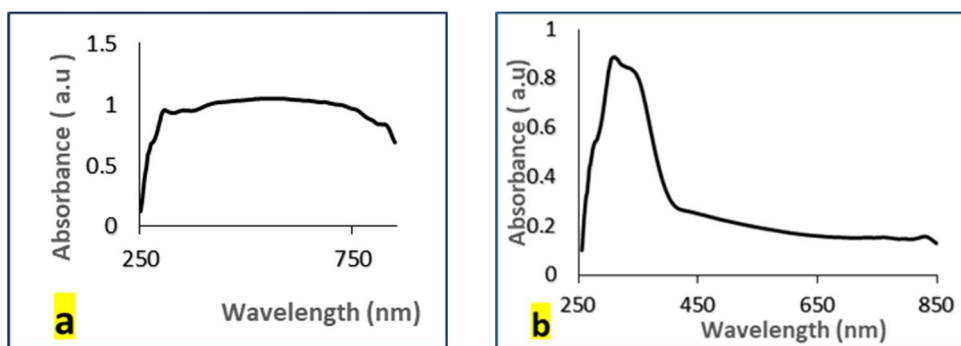


**Figure 7.** UV-Vis Spectrum of (a) CuO, and (b) TiO<sub>2</sub> nanoparticles.

## The DSSCs parameter

The dye- sensitized solar cells (DSSCs) were made of nanomaterials that were prepared and enhanced their efficiency using dyes, and the efficiency was calculated. The following formula was used to calculate the solar cell's energy conversion efficiency ( $\eta$ ):

$$\eta = p_{max}/pin = (Voc \cdot Jsc \cdot FF) / Pin \times 100\% \quad (3)$$

where  $p_{max}$  is the maximum power output,  $Voc$  is photovoltaic open circuit,  $Jsc$  is short circuit density, and  $Pin$  is a lamp power incident, which is equal to  $40 \text{ mW/cm}^2$ . Additionally, the fill factor (FF) is represented by:

$$FF = \frac{V_{max} J_{max}}{Voc Jsc} \quad (4)$$

where  $J_{max}$  is the current density and  $V_{max}$  is the maximum output voltage. The solar cell characteristics are  $Voc$ ,  $Jsc$ ,  $V_{max}$ ,  $J_{max}$ ,  $FF$ , and  $\eta$  for CuO and  $TiO_2$  with chlorophyll and methylene blue dyes provided in Table 1.

**Table 1.** Photo-electrochemical parameters of the DSSCs,  $A=1\text{cm}$  under intensity light  $40 \text{ Mw/cm}^2$ .

<i>NP<sub>s</sub>-Dye</i>	<i>J<sub>sc</sub> (mA)</i>	<i>Voc (V)</i>	<i>J<sub>max</sub> (mA)</i>	<i>V<sub>max</sub> (V)</i>	<i>FF</i>	<i>η %</i>
CuO-Chloropyll	4.8	0.62	2.9	0.36	0.35	2.61
CuO- Methylene B	7.1	0.65	4.1	0.36	0.32	3.69
TiO <sub>2</sub> -Chloropyll	4.3	0.53	2.6	0.32	0.36	2.08
TiO <sub>2</sub> -Methylene B	6.9	0.56	4	0.32	0.33	3.20

Enhancing solar efficiency by using natural dye is attributed to auxochrome groups of chlorophyll dye, such as carbonyl (C=O) groups, which supply the ability to absorb the light in a visible spectrum from the sun. Thus, these

auxochrome groups can be connected to the Cu (II) and Ti (IV) positions of the nanoparticles' surface in favour of electron transfer from the chlorophyll molecules to the CuO and TiO<sub>2</sub> conduction band. In addition, chlorophylls possess a porphyrin ring, which serves as a suitable light-harvesting antenna for assembling solar energy. Consequently, CuO and TiO<sub>2</sub> with porphyrin have been good sensitizers for achieving photocatalysis of visible light.<sup>32</sup> While enhancing solar efficiency by using chemical dye (MB) is due to the occurrence of an electron transfer from the dye to CuO and TiO<sub>2</sub> NPs, the results showed higher efficiency of the MB dye compared to the pigment chlorophyll. This was attributed to the synergetic effect of the phase junction of methylene blue and CuO and TiO<sub>2</sub> NPs, which reduces the recombination of photoexcited electron-hole pairs.<sup>33</sup> Additionally, due to the difficulty of fixing the natural dye on the semiconductor surface, as well as the presence of alkyl and vinyl groups in the structure, this causes a steric barrier that prevents chlorophyll molecules from interacting with CuO and TiO<sub>2</sub> NPs.<sup>34</sup> Finally, since cupric oxide nanoparticles, a photo-generating material, have higher absorption in the visible region and inject excess electrons into the structure, their energy gap is lower, the particle size is small, providing a large surface area for dye absorption on the metal oxide surface, and thus the conversion efficiency is higher compared to titanium oxide nanoparticles.<sup>35</sup> Figure 8 shows the working electrode for the dye-sensitized solar cell, which is based on synthetic CuO and TiO<sub>2</sub> NPs.

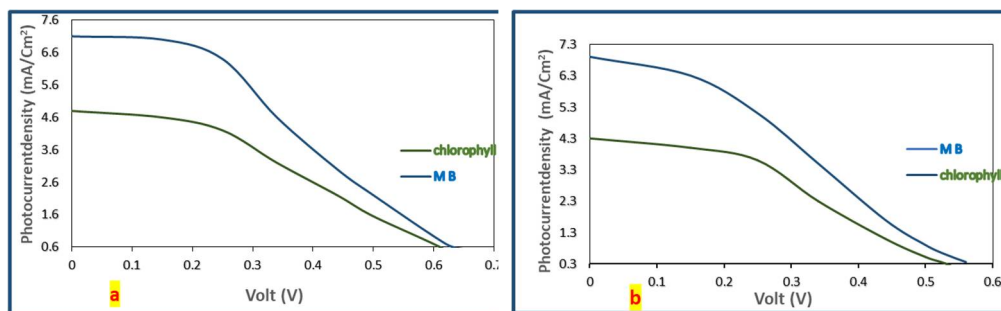


**Figure 8.** J-V curve of (a) CuO, and (b) TiO<sub>2</sub> NPs for the dye-sensitized solar cell.

---

## Conclusion

Dye-sensitized solar cells (DSSCs) with high efficiency in producing electrical energy were prepared from CuO and TiO<sub>2</sub> nanoparticles safely and highly efficiently from available and cheap raw materials and by a safe, easy, and fast electrochemical method. The FESEM and TEM images indicated that samples revealed a well-ordered and good-sized distribution of particles, and the results of the XRD technique showed a nanoparticle synthesized in a small size. Also, the energy band gap was measured by using UV-Visible techniques. Dyes with high sensitivity to light were used to improve the efficiency of the cell, where the efficiency of energy conversion ( $\eta$ ) of ITO-CuO was approximately 3.69 and 2.61% with methylene blue dye and chlorophyll dye, respectively, while the efficiency of ITO-TiO<sub>2</sub> was 3.20 with MB and 2.08% with chlorophyll. The results showed a significant progression in efficiency of energy conversion using methylene blue dye in both cells, and the DSSC using CuO was the best. The possibility of fabricating more efficient cells from natural materials will be investigated in the future.

## Acknowledgements

The authors appreciate all the workers in the laboratories of the Department of Physics / College of the Science / University of Kufa.

## Conflict of Interest

The authors confirm that all figures and tables in the manuscript are ours and that the manuscript has not been sent to another journal.

## Author Contributions

The first researcher contributed to proposing the project idea, interpreting the analytical data, and reviewing the research, and the second researcher contributed to implementing the research project, writing the manuscript, and interpreting the results.

## References

1. O'Regan, B.; Grätzel, M. A low-cost, high-efficiency solar cell based on dye-sensitized colloidal TiO<sub>2</sub> films. *Nature* **1991**, *353*, 737-740.
2. Islam, M. M.; Nafees, A. Nanotechnology for Water Splitting: A Sustainable Way to Generate Hydrogen. In *Modern Nanotechnology*; J.A. Malik, M.J. Sadiq Mohamed, Eds., Springer, Cham., **2023**, *1*, 223-253.
3. Vaz, B.; Pérez-Lorenzo, M. Unraveling structure–performance relationships in porphyrin-sensitized TiO<sub>2</sub> photocatalysts. *Nanomater.* **2023**, *13*(6), 1097.
4. Koudjina, S.; Kumar, V.; Atohou, G. Y.; Gbenou, J. D.; Chetti, P. Impact of organic dye-photosensitizer on TiO<sub>2</sub> nanocrystalline surface for high performance organic electronic devices: A computational insight. *J. Photochem. Photobiol. A.* **2023**, *442*, 114772.
5. Al-Horaibi, S.A.; Al-Odayni, A.B.; Alezzy, A.; ALSaedy, M.; Al-Adhrai, A.; Saeed, W.S.; Hasan, A. Novel Squaraine Dyes for High-Performance in Dye-Sensitized Solar Cells: Photophysical Properties and Adsorption Behavior on TiO<sub>2</sub> with Different Anchoring Groups. *J. Mol. Struct.* **2023**, *1290*, 135943.
6. Karthikeyan, B.; Gnanakumar, G.; Alphonsa, A.T. Future is on Cheap Metal Oxides-A Review. *Nano-Met. Oxides* **2023**, 111-120.
7. Bibi, S.; Shah, S. S.; Muhammad, F.; Siddiq, M.; Kiran, L.; Aldossari, S. A.; Mushab, M. S. S.; Sarwar, S. Cu-doped mesoporous TiO<sub>2</sub> photocatalyst for efficient degradation of organic dye via visible light photocatalysis. *Chemosphere* **2023**, *339*, 139583.
8. Yadeta, T. F.; Imae, T. Effect of Carbon Dot on Photovoltaic Performance of n-TiO<sub>2</sub>/p-NiO and n-TiO<sub>2</sub>/p-CuO Heterojunctions in Dye-Sensitized Solar Cells. *Appl. Surf. Sci.* **2023**, *637*, 157880.
9. Maurya, I. C.; Gupta, A. K.; Srivastava P.; Bahadur, L. Callindra haematocephata and Peltophorum pterocarpum flowers as natural sensitizers for TiO<sub>2</sub> thin film based dye-sensitized solar cells. *Opt. Mater.* **2016**, *60*, 270-276.
10. Pandey, A. K.; Ahmad, M. S.; Rahim, N. A.; Tyagi, V. V.; Saidur, R. Natural sensitizers and their applications in dye-sensitized solar cell. In *Environ.*

- biotechnol: for sustainable future*; R. Sobti, N. Arora, R. Kothari, Eds., Springer, Singapore, **2019**, 375-401.
11. Lin, Ji.; Jiaying, Li.; Jinghua, Lei.; Yuanyuan, Ren.; Shuyu, Zhou.; Lihua, Li. Preparation and characterization of Cu<sup>2+</sup>/ZnO/TiO<sub>2</sub> nanocomposites for the treatment of typical benzene series in oilfield produced water. *Catal. Commun.* **2023**, *174*, 106572.
  12. Buu, T. T.; Son, V. H.; Nam, N. T. H.; Hai, N. D.; Vuong, H. T.; Dat, N. M.; Lin, T. H.; Phong, M. T.; Hieu, N. H. Three-dimensional ZnO–TiO<sub>2</sub>/graphene aerogel for water remediation: the screening studies of adsorption and photodegradation. *Ceram. Int.* **2023**, *49(6)*, 9868-9882.
  13. Jiang, T.; Bujoli-Doeuff, M.; Farré, Y.; Pellegrin, Y.; Gautron, E.; Boujtita, M.; Cario, L.; Jobic, S.; Odobel, F. CuO nanomaterials for p-type dye-sensitized solar cells. *RSC Adv.* **2016**, *6(114)*, 112765-112770.
  14. Kumar, A.; Gangawane, K. M. Synthesis and effect on the surface morphology & magnetic properties of ferrimagnetic nanoparticles by different wet chemical synthesis methods. *Powder Technol.* **2022**, *410*, 117867.
  15. Omar, A.; Ali, M. S.; Abd Rahim, N. Electron transport properties analysis of titanium dioxide dye-sensitized solar cells (TiO<sub>2</sub>-DSSCs) based natural dyes using electrochemical impedance spectroscopy concept: A review. *Sol Energy* **2020**, *207*, 1088-1121.
  16. Sharma, J. K.; Akhtar, M. S.; Ameen, S.; Srivastava, P.; Singh, G. Green synthesis of CuO nanoparticles with leaf extract of *Calotropis gigantea* and its dye-sensitized solar cells applications. *J. Alloys Compd.* **2015**, *632*, 321-325.
  17. Rasheed, A.; Ibrahim, A. I.; Reaad, S.; Kadhim, M. M. Synthesis and Characterization of CuO Nanoparticles for Increase the Efficiency of the photovoltaic cell. *Egypt. J. Chem.* **2023**, *66(1)*, 49-53.
  18. Singh, L. K.; Koiry, B. P. Natural dyes and their effect on efficiency of TiO<sub>2</sub> based DSSCs: a comparative study. *Mater. Today: Proc.* **2018**, *5(1)*, 2112-2122.
  19. Arulraj, A.; Senguttuvan, G.; Veeramani, S.; Sivakumar, V.; Subramanian, B. Photovoltaic performance of natural metal free photo-sensitizer for TiO<sub>2</sub> based dye-sensitized solar cells. *Optik.* **2019**, *181*, 619-26.

20. Micó-Vicent, B.; Perales Romero, E.; Jordán-Núñez, J.; Viqueira, V. Halloysite and laponite hybrid pigments synthesis with copper chlorophyll. *Appl. Sci.* **2021**, *11*(12), 5568.
21. How, Y.Y.; Numan, A.; Mustafa, M. N.; Walvekar, R.; Khalid, M.; Mubarak, N.M. A review on the binder-free electrode fabrication for electrochemical energy storage devices. *J. Energy Storage.* **2022**, *51*, 104324.
22. El-Khawaga, A. M.; Zidan, A.; Abd El-Mageed, A. I. Preparation methods of different nanomaterials for various potential applications: A Review. *J. Mol. Struct.* **2023**, *1281*, 135148.
23. Anand, A.; Mittal, S.; Leeladevi, V.; De, D. Nanoflower shaped ZnO photoanode and natural dye sensitizer based solar cell fabrication. *Mater. Today: Proc.* **2023**, *72*, 227-231.
24. Rheima, A. M.; Hussain, D. H.; Abed, H. J. Fabrication of a new photo-sensitized solar cell using TiO<sub>2</sub>/ZnO nanocomposite synthesized via a modified sol-gel Technique. *IOP Conf. Ser.: Mater. Sci. Eng.* **2020**, *928*(5), 052036.
25. Verma, B.; Sahni, M.; Gupta, A.; Thakur, A.; Chauhan, S.; Agarwal, D. Effect of Pr/Ni Co-dopants on surface chemical bonding states of BiFeO<sub>3</sub> nanoparticles with promising magnetic and photocatalytic properties. *J. Electron. Mater.* **2023**, *52*, 1-8.
26. Yu, S.; Jia, X.; Yang, J.; Wang, S.; Li, Y.; Song, H. Highly sensitive ethanol gas sensor based on CuO/ZnSnO<sub>3</sub> heterojunction composites. *Mater. Lett.* **2021**, *291*, 129531.
27. Zhao, H. Y.; Kuang, J. L.; Sun, P.; Liu, W. X.; Cao, W. B. One-Step hydrothermal synthesis of an orthorhombic WO<sub>3</sub>·H<sub>2</sub>O/TiO<sub>2</sub> heterojunction and its photocatalytic activity. *Mater. Sci. Forum.* **2022**, *1072*, 195-201.
28. Yu, Y. H.; Chen, Y. P.; Cheng, Z. Microwave-assisted synthesis of rod-like CuO/TiO<sub>2</sub> for high-efficiency photocatalytic hydrogen evolution. *Int. J. Hydrog. Energy.* **2015**, *40*(46), 15994-16000.
29. Kubiak, A.; Bielan, Z.; Kubacka, M.; Gabała, E.; Zgoła-Grześkowiak, A.; Janczarek, M.; Zalas, M.; Zielińska-Jurek, A.; Siwińska-Ciesielczyk, K.; Jesionowski, T. Microwave-assisted synthesis of a TiO<sub>2</sub>-CuO heterojunction

- with enhanced photocatalytic activity against tetracycline. *Appl. Surf. Sci.* **2020**, *520*, 146344.
30. Tauc, J. Optical properties and electronic structure of amorphous Ge and Si. *Mater. Res. Bull.* **1968**, *13(1)*, 37-46.
31. Mancuso, A.; Blangetti, N.; Sacco, O.; Freyria, F. S.; Bonelli, B.; Esposito, S.; Sannino, D.; Vaiano, V. Photocatalytic degradation of crystal violet dye under visible light by Fe-Doped TiO<sub>2</sub> prepared by Reverse-Micelle Sol–Gel method. *Nanomater.* **2023**, *13(2)*, 270.
32. Krishnan, S.; Srivastava, A. Application of TiO<sub>2</sub> nanoparticles sensitized with natural chlorophyll pigments as catalyst for visible light photocatalytic degradation of methylene blue. *J. Environ. Chem. Eng.* **2021**, *9(1)*, 104699.
33. Buu, T. T.; Son, V. H.; Nam, N. T. H.; Hai, N. D.; Vuong, H. T.; Dat, N. M.; Lin, T. H.; Phong, M. T.; Hieu, N. H. Three-dimensional ZnO–TiO<sub>2</sub>/graphene aerogel for water remediation: the screening studies of adsorption and photodegradation. *Ceram. Int.* **2023**, *49(6)*, 9868-9882.
34. Munandar, M. R.; Hakim, A. S. R.; Puspitadinda, H. A.; Andiyani, S. P.; Nurosyid, F. The effect of mixing Chlorophyll-Antocyanin as a natural source dye on the efficiency of dye-sensitized solar cell (DSSC). *J. Phys.: Conf. Ser.* **2022**, *2190(1)*, 012042.
35. Siddiqui, H.; Parra, M. R.; Pandey, P.; Qureshi, M. S.; Haque, F. Z. Utility of copper oxide nanoparticles (CuO-NPs) as efficient electron donor material in bulk-heterojunction solar cells with enhanced power conversion efficiency. *J. Sci.: Adv. Mater. Devices.* **2020**, *5(1)*, 104-110.